Dual-wavelength semiconductor laser with 191 nm mode spacing

Chi-Chia Huang[a] and Ching-Fuh Lin [a, b]
[a] Graduate Inst. of Electron-Optical Engr., National Taiwan Univ., Taiwan
[b] Dept. of Electrical Engr. and Graduate Inst. of Electronics Engr., National Taiwan Univ., Taiwan

ABSTRACT

A very wide tuning range of dual-wavelength semiconductor lasers with properly designed nonidentical InGaAsP quantum wells is reported. By well aligning the external cavity, the dual-wavelength operation can be achieved with a record wavelength separation about 191 nm (27.4 THz) at 22.7°C. The wide separation of two wavelengths is possible due to a proper modification of the external-cavity configuration and reduced gain competition of laser modes.

Keywords: broadband, competition, dual-wavelength, external cavity, nonidentical multiple quantum wells, semiconductor laser, wavelength separation.

1. INTRODUCTION

Dual-wavelength laser systems have many potential applications in optic-electronics such as two-wavelength interferometry, wavelength-division multiplexing (WDM) communication system, laser spectroscopy, differential lidar, optical data processing, and so on. In the past, many approaches have been used to achieve simultaneous two-wavelength oscillation in both fiber and semiconductor lasers. For example, in fiber lasers, Takahashi *et al.* has used an array of doped fiber amplifiers as a multiple wavelength source [1], and Battiato *et al.* has used a codoped fiber laser as a common gain medium in a linear cavity for dual-wavelength operation [2]. In semiconductor lasers, the common approach for multiple wavelength operation is using array of lasers with physically separated gain media for each wavelength [3], [4]. Dual-wavelength operation with a single semiconductor gain medium has also been achieved by Lin *et al.* [5] and Hidaka *et al.* [6]. The use of a single gain medium shared by both wavelengths has the advantage of simplicity because no elaborate fabrication and packaging procedures are required [7]. However, the tuning range is usually small in a dual-wavelength laser system with single gain medium because a broadband gain medium is not easy to design.

Under dual-wavelength operation, some sort of mode competition will occur, especially when the mode spacing is small [5], [8]. Mode competition can cause drastic variation of the power difference between the oscillation modes even if the relative external loss of the two modes only makes a small change. Therefore, it is hard to achieve simultaneous two-wavelength oscillation with almost the same intensity at both wavelengths. That is, the difficulty for two-mode oscillation at small mode spacing is caused by mode competition. However, when the mode spacing is large enough, mode competition is significantly reduced [9], increasing the possibility of two-mode oscillation. On the other hand, the difficulty for dual-wavelength operation at very large mode spacing is caused by the limited bandwidth of the gain medium and the difficulty of optical-path alignment in the external cavity. In addition, the operation current and temperature should also be carefully adjusted. In this article, we report record mode spacing as large as 191 nm (1350.3 nm~1541.3 nm) in dual-wavelength semiconductor lasers with single gain medium. The wide range of dual-wavelength operation indicates that the laser system has the potential for operation at several wavelengths simultaneously. This could dramatically lower the cost and simplify the system when the laser system is used for WDM applications. Further increase of the mode spacing with the same device would be possible if the efficiency of the optical components in the external cavity is increased.

2. EXPERIMENT

2.1 Broadband gain medium design

Novel In-Plane Semiconductor Lasers III, edited by Claire F. Gmachl, David P. Bour,
Proceedings of SPIE Vol. 5365 (SPIE, Bellingham, WA, 2004) · 0277-786X/04/$15 · doi: 10.1117/12.525582

To obtain a wide tuning range, a broadband superluminescent diode (SLD) is the prerequisite. Quantum-well (QW) engineering is a convenient and widely used approach to broaden the bandwidth of SLDs. This scheme includes using a single QW with simultaneous transition s of n = 1 and n = 2 states [10,11], and using nonidentical QWs [12-15]. Because the simultaneous transitions of n = 1 and n = 2 energy states in identical QWs rely strongly on the device lengths [10,11], nonidentical multiple quantum wells (MQWs) were recently been widely used for broadband purposes.

However, theoretically analysis has predicted that carrier distribution among the MQWs is nonuniform [16,17]. Experimental evidence of this phenomenon was also indirectly obtained from the characteristics of laser diodes [18,19]. Nonuniform carrier distribution means that each QW of the MQW structure accumulates a different number of carriers, so their corresponding emission intensities are not equal. Thus, the overlap of the individual spectrum from each type of QW, weighed by its corresponding emission intensity, does not directly result in a broadband spectrum. Therefore, the design of nonidentical MQW structures for broadband purposes is not intuitively straightforward, and more studies on the spectral behavior of the ninidentical MQWs are necessary.

Consider the three different QW structures shown in Fig. 1. A separate confinement heterostructure (SCH) is formed in connection with the wells. The SCH layer has a thickness of 120 nm. The wells are separated by 15-nm-wide $In_{0.86}Ga_{0.14}As_{0.3}P_{0.7}$ barriers. All the three samples have two 8.7-nm $In_{0.53}Ga_{0.47}As$ QWs and three 6.0-nm $In_{0.67}Ga_{0.33}As_{0.72}P_{0.28}$ QWs. In sample A, the three 6.0-nm $In_{0.67}Ga_{0.33}As_{0.72}P_{0.28}$ QWs are placed near the n-cladding layer, whereas the two 8.7-nm $In_{0.53}Ga_{0.47}As$ QWs are placed near the p-cladding layer. Sample B has the opposite sequence. In sample C, each $In_{0.53}Ga_{0.47}As$ QW is placed between the $In_{0.67}Ga_{0.33}As_{0.72}P_{0.28}$ QWs. The emission energies of the 6.0-nm $In_{0.67}Ga_{0.33}As_{0.72}P_{0.28}$ QW and 8.7-nm $In_{0.53}Ga_{0.47}As$ QW were calculated using the Luttinger-Kohn method [20]. Table I shows the emission wavelengths corresponding to the calculated energy levels. $In_{0.67}Ga_{0.33}As_{0.72}P_{0.28}$ QWs and $In_{0.53}Ga_{0.47}As$ QWs have three and two quantized energy levels, respectively.

For sample A, emission at low injection current occurs at the wavelength corresponding to the n = 1 transition in the 8.7-nm $In_{0.53}Ga_{0.47}As$ QWs, which are close to the n-cladding layer. When the injection current increases, the emission spectrum is broadened owing to the simultaneous transitions of n = 1 and n = 2 states. The emission contribution from the 6.0-nm $In_{0.67}Ga_{0.33}As_{0.72}P_{0.28}$ QWs is obvious only when the injection current is very large. For sample C, emission also first occurs at the wavelength corresponding to the n = 1 transition in the 8.7-nm $In_{0.53}Ga_{0.47}As$ QWs when the injection current is very low. Similar to sample A, increasing the injection current induces simultaneous transitions of the n = 1 and n = 2 states. However, the threshold current for emission corresponding to the

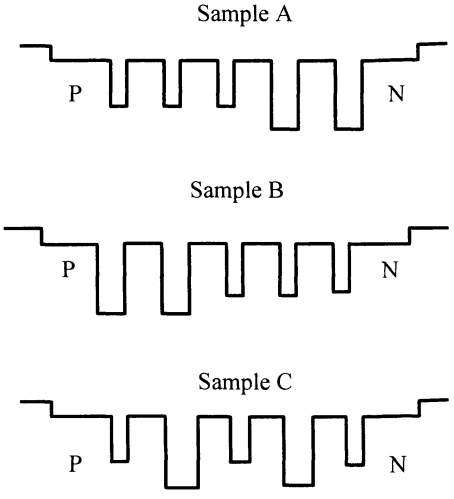

Fig. 1. Designed QW structures: wide QW, $In_{0.53}Ga_{0.47}As$, 8.7 nm; narrow QW, $In_{0.67}Ga_{0.33}As_{0.72}P_{0.28,\ 6.0\ nm}$, 6.0 nm; barrier, $In_{0.86}Ga_{0.14}As_{0.3}P_{0.7}$, 15 nm; SCH region, $In_{0.86}Ga_{0.14}As_{0.3}P_{0.7}$, 120nm.

TABLE I. Calculated Transition Wavelengths Corresponding to the Bounded Energy States of the Nonidentical MQWs of the Designed SLD

n	8.7-nm $In_{0.53}Ga_{0.47}As$ Double QW (μm)	6.0-nm $In_{0.67}Ga_{0.33}As_{0.72}P_{0.28}$ Triple QW (μm)
1	1.54	1.3
2	1.46	1.24
3	1.18	Unbounded

$In_{0.67}Ga_{0.33}As_{0.72}P_{0.28}$ QWs is lower for sample C than for sample A. Further increase of the injection current causes the emission corresponding to the n = 1 transition in the $In_{0.67}Ga_{0.33}As_{0.72}P_{0.28}$ QWs to grow significantly. Therefore, the spectral width of sample C is smaller than that of sample A. For sample B, emission at low injection current occurs at the wavelength corresponding to the n = 1 transition in the 6.0-nm $In_{0.67}Ga_{0.33}As_{0.72}P_{0.28}$ QWs, which are also close to the n-cladding layer. Further increase of the injection current does not obviously change the emission wavelength. Therefore, sample B has the narrowest spectral width.

The emission characteristics described above are obviously related to the sequential capture of carriers by the MQWs. When the devices are forward biased, electrons are injected from the n-cladding layer and holes are injected from the p-cladding layer. These carriers are then captured by the QWs in the order that the carriers encounter them. According to the experimental results discussed above, the wells near the n-cladding layer trap most of the carriers. Therefore, the 8.7-nm $In_{0.53}Ga_{0.47}As$ QWs near the n-cladding layer (sample A) contribute to the emission first. When injection current increases, the carriers overflow to $In_{0.67}Ga_{0.33}As_{0.72}P_{0.28}$ QWs. Theoretical calculation shows that the total gain of the three $In_{0.67}Ga_{0.33}As_{0.72}P_{0.28}$ QWs increases much faster than that of the two $In_{0.53}Ga_{0.47}As$ QWs for large numbers of injected carriers. Thus the three $In_{0.67}Ga_{0.33}As_{0.72}P_{0.28}$ QWs dominate the emission when the injection current is large. Similarly, sample C has emission that is dominated by the three $In_{0.67}Ga_{0.33}As_{0.72}P_{0.28}$ QWs when the injection current is large. However, because some $In_{0.67}Ga_{0.33}As_{0.72}P_{0.28}$ QWs of sample C are closer to the n-cladding layer, the corresponding emission occurs at a lower injection current than sample A. This phenomenon reveals that the carrier distribution also depends on the injected carrier level. For sample B, because all three $In_{0.67}Ga_{0.33}As_{0.72}P_{0.28}$ QWs are close to the n-cladding layer, they have significant gain for emission regardless of the current level.

In our experiment, we use the MQW structure as in sample A, and use laser diodes (LDs) with straight waveguide. This is because that, compared with the tilt or bent waveguide SLDs, the straight one has lower loss and lower threshold current. This can facilitate the tuning of the long-wavelength mode because the long-wavelength mode is very loss-sensitive. The length of the device was about 300 μm. No facet coatings were applied to the device. The measured emission spectrum of the LD is shown in Fig. 2. The bandwidth of the emission spectrum is limited by the Fabry-Perot resonance of the straight waveguide.

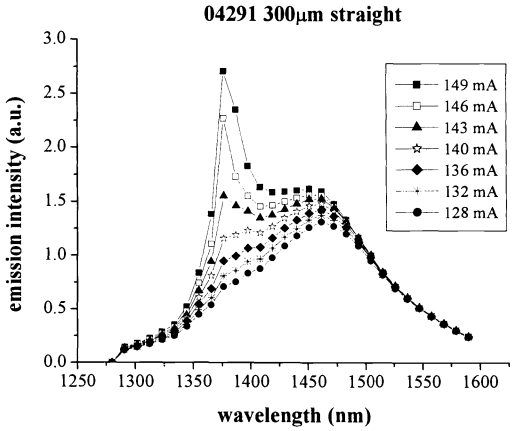

Fig. 2. Measured emission spectrum of the SLD

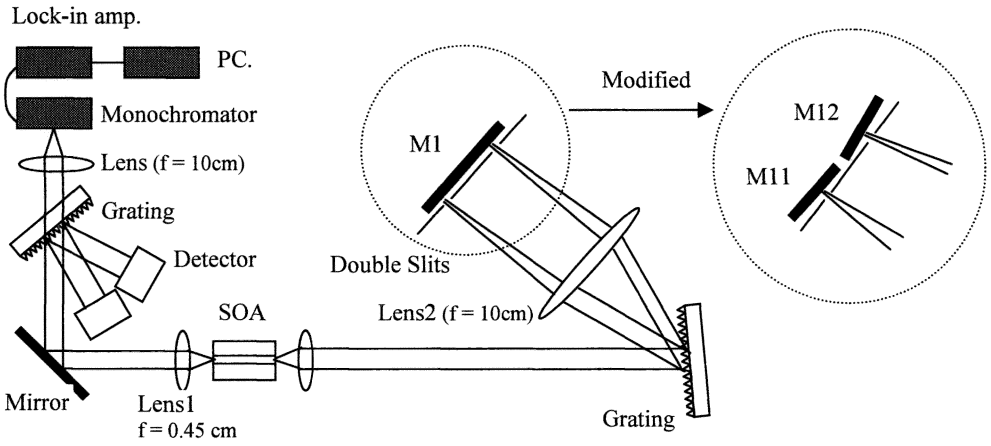

Fig. 3. Experimental setup (1)

2.2 External cavity and operation condition

The experimental setup is shown in Fig. 3. Two collimators with f = 4.5 mm and NA = 0.55 are used to collimate the light beams emitted from two facets of the SLD. The coupling efficiency of the collimators is about 70%. The grating is 600 lines/mm and is Au-coated. Its efficiency is about 80%. A lens with f = 10 cm is placed at 10 cm from both the grating and the mirror M1. The linear external cavity is of reflected-type grating telescope configuration. However, the exact alignment of lens (Lens2) position between the grating and the mirror M1 is difficult, leading to the light beams of different wavelengths between Lens2 and M1 usually not parallel. The deviation from the parallel direction is particularly severe when the two wavelengths are widely separated. Thus it is impossible to use a single mirror M1 for the simultaneous reflection of both light beams for dual-wavelength operation with large spectral spacing. To overcome the alignment difficulty, we used two mirrors for the long wavelength and the short wavelength, respectively, as shown in the modified insert of Fig. 3. The maximum mode spacing that can be achieved with this setup is about 170 nm, as demonstrated in [21].

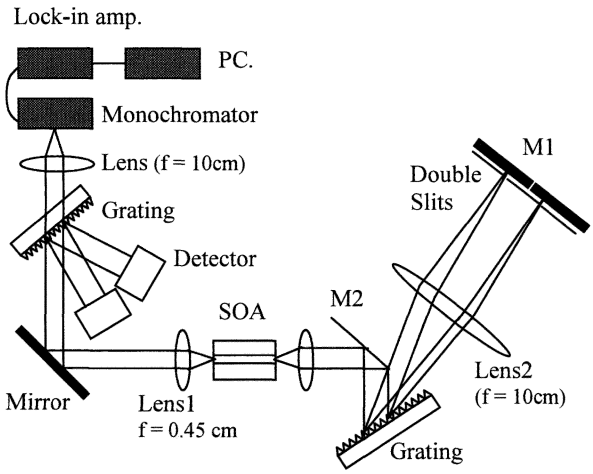

Fig. 4. Experimental setup (2)

To obtain a more efficient external cavity, we again make several modifications to the setup in Fig. 3. The first one is the introduction of the mirror M2 (see Fig. 4). According to the grating principle, the beams of different wavelengths are horizontally dispersed at the mirror with a spatial separation $W \sim L(1/\Lambda)(1/\cos\theta_R)\Delta\lambda$, where $\Delta\lambda$ is the spectral separation, Λ is the grating period, θ_R is the first-order diffraction angle, and L is the distance between the lens and the grating. To obtain better diffraction efficiency, θ_R must be as small as possible. However, if θ_R is too small, the path of the input beam and the diffracted beam will be closely separated, and the holding stages of lens2 and mirror M1 will block the path of the input beam. Therefore, we introduce an additional mirror M2 into the cavity and put the lens and M1 behind M2 to avoid blocking the input beam. To obtain minimum θ_R, the light beam must be carefully aligned so that it passes just through the rim of mirror M2. Experiment shows that this is a critical step determining the tuning range of the long-wavelength mode. An increase of θ_R about several degrees can lead to tens of nanometer decrease in the tuning range.

The second modification is the optical path of the two wavelengths through Lens2. This modification is very tricky, and has to be tried many times through experiment. Experiments show that the optimized optical path has three different types, depending on the wavelength separation of the two modes. In general, at mode spacing smaller than 100 nm, we should let both two wavelengths passing through the high transmission center of lens2 as near as possible. Usually, we pass the middle wavelength of these two modes through the center of Lens2. However, when the mode spacing is increased to 174 nm, the spatial separation of the two modes will be about 1.5 cm. It means that the light will pass through a path away from the center of Lens2, which is of diameter 5 cm. Deviation of the light beam from the lens center greatly increases the loss. Although the loss in the short-wavelength mode can be compensated by increasing the injection current, the gain of the long-wavelength mode is reduced at the same time due to heating effect. Therefore, in this condition, we make the long-wavelength mode nearly pass through the high transmission center of Lens2. At mode spacing 191 nm, the paths of the two wavelengths need to be readjusted. This is because that, at mode spacing 191 nm, mode anti-competition is very severe [9], and the loss thus introduced to the short-wavelength mode is very large. Moreover, anti-competition can provide the long-wavelength mode with some optical gain. Therefore, in this condition, we should pass the short-wavelength mode nearly through the high transmission center of Lens2.

The operation current and temperature should also be carefully adjusted. First, since we use LD with straight waveguide, the operation current should not be much larger than the threshold current, which is 143 mA at 22.7 °C. Otherwise, the Fabry-Perot mode will start oscillating and suppress other modes selected by the external-cavity configuration. Our operation current is 3 mA larger than the threshold current. This is acceptable because the slight oscillation of the Fabry-Perot mode will be suppressed by the short-wavelength (SW) mode through mode competition. Second, although low temperature is favorable for the oscillation of the long-wavelength (LW) mode, it will also lower the threshold current of the Fabry-Perot mode, leading the oscillation dominated by this mode. An optimal temperature thus exists at fixed current level for which the oscillation of the Fabry-Perot mode is negligible. Therefore, the operation current and temperature need to be experimented many times for maximum tuning range. In our experiment, the operation current is 146 mA, and the temperature is 22.7 °C. There might be another choice of the operation and temperature for very broad separation of the dual wavelength. However, within our experimental time, we did not discover.

At the laser output, we use a grating to separate the light beam and use two detectors to measure the light power of each mode. Afterwards, we remove the grating and the detectors and use the monochromator to measure the spectrum.

2.3 Experimental results

Fig. 4 shows the dual-wavelength spectrum of the maximum mode spacing. The mode spacing is about 191 nm, which corresponds to 27.4 THz in frequency. The SW mode is at 1350.3 nm and LW mode is at 1541.3 nm. This is the maximum mode spacing under which we can see two separate lasing peaks in the spectrum. Detailed spectrum for each mode is also shown in the figure. The FWHM of each lasing mode is less then 0.36nm. The double-slit we used has a V shape, with the LW side vertically straight and the SW side tilted at an angle of 30° from the vertical line. Because it is difficult to make the effective width of the tilted slit small, the spectrum of the SW mode usually contains two peaks. As the mode spacing is decreased by 2.9 nm with respect to Fig. 4, the light intensities of the SW and the LW modes are nearly doubled and tripled, respectively. The spectra for three different mode spacing are shown in Fig. 5, and are plotted together for comparison. From Fig. 5, we can see that although the output power at 191 nm mode spacing is small, it could increase very fast with the reduction of the mode spacing. Light power of the two modes at different

mode spacing in Fig. 5 is listed in Table II. The smallest mode spacing that can be tuned is less than 10 nm in our external-cavity configuration. Also, at a fixed mode spacing, we can randomly choose the position of the two modes from 1350.3 nm to 1541.3 nm as long as the balance between the gain and the loss is properly adjusted. That is, there is no 'gap' where dual-wavelength operation is forbidden.

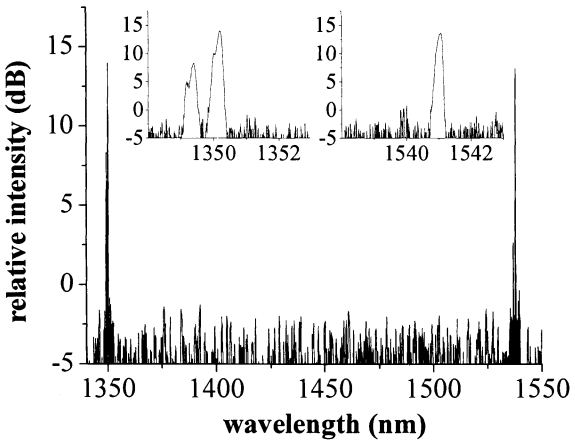

Fig. 4. Spectrum of maximum mode spacing. The SW and LW mode are located in 1350.3 nm and 1541.3 nm, respectively

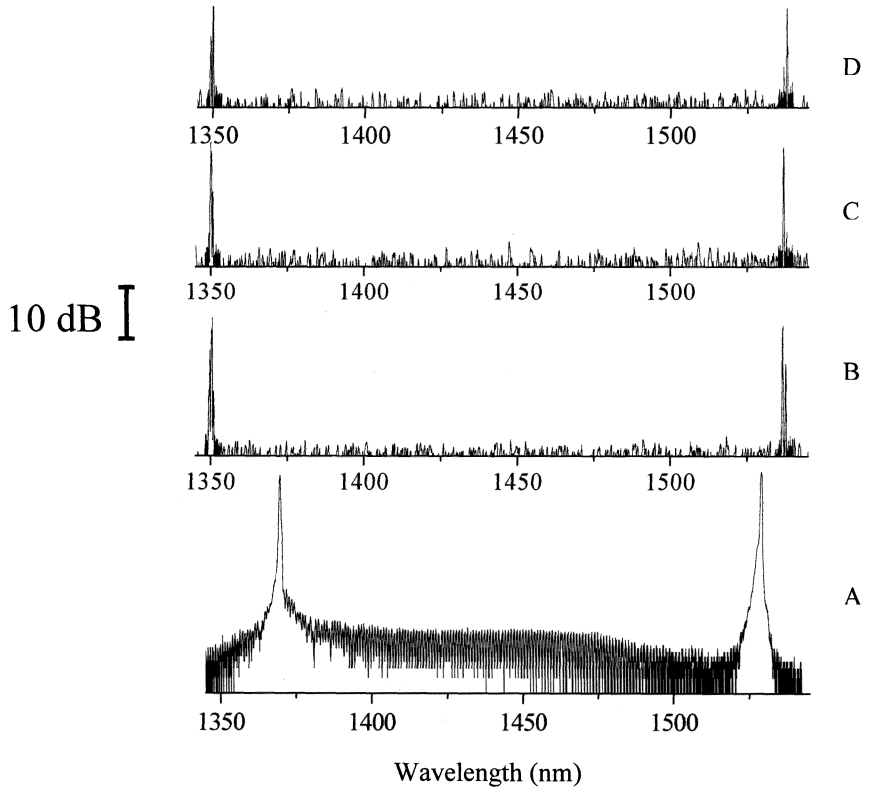

Fig. 5. Spectra of different mode spacing. A 159.1 nm (1371.0 nm and 1530.1 nm), B 181.5 nm (1356.4 nm and 1537.9 nm), C 188.1 nm (1352.1 nm and 1540.2 nm), D 191 nm (1350.3 nm and 1541.3 nm).

TABLE II Output power of the short-wavelength mode (PS) and output power of the long-wavelength mode (PL) at different mode spacing (SP).

SP (nm)	PS (mW)	PL (mW)
191	0.157	0.176
188.1	0.272	0.563
181.5	0.604	0.930
159.1	0.30	0.42

When the mode spacing is very large, as shown in Fig. 4, the side-mode suppression ratio (SMSR) is about 13 dB. As the mode spacing is less than 181nm, the SMSR is larger than 20dB. The spectrum between the two lasing modes is very flat. It is the noise level of the measurement system. The power of amplified spontaneous emission (ASE) or spontaneous emission is actually than this level. Due to the instrumentation noise, the ratio of the optical power of the lasing modes to the total noise power in spectra B, C, D of Fig. 5 seems to be low. However, when we increase the signal to noise ratio of the measurement system, we found that the SMSR is larger than 27 dB, as shown in spectrum A of Fig. 5. In this curve, the ASE and spontaneous emission varies with the wavelength. After our calculation from spectrum A in Fig.5, 38% of the total power belongs to the mode 1371.0 nm, and 52% belongs to the mode 1530.1 nm. Therefore, the power of each mode was about 9.5 dB larger than the total ASE noise. The ASE noise is very small. The reason for the small ASE power is as follows. The broadband SLD spreads out the spontaneous emission power to a very broad spectral range. This leads to the power of the lasing mode returned by the grating much larger than the power of other spectral range. Therefore, the lasing mode has much stronger gain-competition ability than light at other spectral range, so ASE noise is significantly suppressed.

The possibility of large mode spacing is due to the following reasons. First, as discussed above, the gain spectrum of the nonidentical MQWs is broad. Second, at large mode spacing, the two wavelengths are nearly contributed from two different QWs. Therefore, competition at large mode spacing is weak because the carrier transportation between QWs is a relatively slow process, compared to the intraband relaxation in the same well. In reality, at mode spacing 191 nm, anti-competition plays a more important role than competition in the laser system [9]. As discussed above, anti-competition can provide the long-wavelength mode with some optical gain. This can help balancing the loss encountered by the long-wavelength mode. Therefore, anti-competition also contributes to our achievement of a broadband tuning range. Further broadening of the mode spacing would be possible with better alignment of the optical components in the external cavity. This could be achieved by adding some feedback control system to the holding stages of the optical components in the cavity instead of manual alignment.

3. Conclusion

Broadband tuning range of dual-wavelength operation is achieved using semiconductor laser with single gain medium. MQW engineering is used to design a gain medium for broadband purpose. Since the carrier distribution in MQWs is nonuniform, the design of nonidentical MQW structures for broadband purposes is not intuitively straightforward, so delicate study of the QW structure and carrier distribution is required for the broadband purpose. In addition, when the broadband gain medium is used, the operation current and temperature should also be carefully adjusted. LD with straight waveguide is used because it has lower loss and lower threshold current, compared with the tilt or bent waveguide. This can facilitate the tuning of the loss-sensitive long-wavelength mode. Oscillation of the Fabry-Perot mode is negligible because it will be suppressed by the short-wavelength mode through mode competition. The external cavity is of reflected-type grating telescope configuration. However, at different mode spacing, different modifications should be applied to the external cavity configuration, such as the optical path of the two modes and the alignment of the feedback mirror. A record mode spacing as large as 191 nm is achieved using the broadband gain medium and the specially designed cavity configuration. Under this large mode spacing, competition between the two modes is weak because the carrier transportation between QWs is a slow process. Moreover, anti-competition dominates the laser system at this mode spacing. This can also help us achieving this record mode spacing. Further broadening of the mode spacing is possible with better alignment of the optical components in the external cavity.

REFERENCES

[1] H. Takahashi, H. Toba, and Y. Inoue, "Multiwavelength ring laser composed of EDFAs and an arrayed-waveguide wavelength multiplexer," *Electron. Lett.* **30**, 44 (1994).

[2] J. M. Battiato, T. F. Morse, and R. K. Kostuk, "Dual wavelength common cavity co-doped fiber laser," *IEEE Photon. Technol. Lett,* **9**, 913 (1997).

[3] K. O. Nyairo, I. H. White, C. J. Armistead, and P. A. Kirkby, "Multiple channel signal generation using a multichannel grating cavity laser with crosstalk compensation," *Electron. Lett.* **28**, 261 (1992).

[4] K. R. Poguntke, J. B. D. Soole, A. Scherer, H. P. LeBlanc, C. Caneau, R. Baht, and M. A. Koza, "Simultaneous multiple wavelength operation of a multistripe array grating integrated cavity laser," *Appl. Phys. Lett.* **62**, 2024 (1993).

[5] C.-F. Lin, M.-J Chen, and B.-L Lee, "Wide-range tunable dual-wavelength semiconductor laser using asymmetric dual quantum wells," *IEEE Photon. Technol. Lett.* **10**, 1208 (1998).

[6] T. Hidaka and Y. Hatano, "Simultaneous two wave oscillation LD using biperiodic binary grating," *Electron. Lett.* **27**, 1075 (1991).

[7] C. L. Wang and C. L. Pan, "Tunable dual-wavelength operation of a diode array with an external grating-loaded cavity," *Appl. Phys. Lett.* **64**, 3089 (1994).

[8] P.-C. Ku, C.-F. Lin, and B.-L. Lee, "Multiple cross switching in a two-mode semiconductor laser," *Appl. Phys. Lett.* **69**, 3984 (1996).

[9] C.-F. Lin, C.-C. Huang, F.-H. Chu, and Y.-S. Su, "Anticompetition of laser modes," *Appl. Phys. Lett.* **82**, 3611 (2003).

[10]A. T. Semenov, V. R. Shidlovski, and S. A. Safin, "Extremely broadband AlGaAs/GaAs superluminescent diodes," *Electron. Lett.* **29**, 854 (1993).

[11]T.R. Chen, L. Eng, Y. H. Zhuang, and A. Yariv, "Quantum well superluminescent diode with very wide emission spectrum," *Appl. Phys. Lett.* **56**, 1345 (1990).

[12]C.-F. Lin, B.-L. Lee, and P.-C. Lin, "Broadband superluminescent diodes fabricated on a substrate with asymmetric dual quantum wells," *IEEE Photon. Technol. Lett.* **8**, 1456 (1996).

[13]X. Zhu, D. Cassidy, M. Hamp, D. Thompson, B. Robinson, Q. Zhao, and M. Davies, "1.4μm InGaAsP-InP strained multiple-quantum-well laser for broad-wavelength tunability," *IEEE Photon. Technol. Lett.* **9**, 1202 (1997).

[14]H. S. Gingrich, D. R. Chumney, S.-Z. Sun, S. D. Hersee, L. F. Lester, and S. R. Brueck, "Broadly-tunable external cavity laser diodes with staggered thickness multiple quantum wells," *IEEE Photon. Technol. Lett.* **9**, 155 (1997).

[15]C.-F. Lin and B.-L. Lee, "Extremely broadband AlGaAs/GaAs superluminescent diodes," *Appl. Phys. Lett.* **71**, 1598 (1997).

[16]N. Tessler and G. Eisenstein, "On carrier injection and gain dynamics in quantum well lasers," *IEEE J. Quantum Electron.* **29**, 1586 (1993).

[17]R. Nagarajan, T. Fukushima, S. W. Corzine, and J. E. Bowers, "Effects of carrier transport on high-speed quantum well lasers," *Appl. Phys. Lett.* **59**, 1835 (1991).

[18]H. Yamazaki, A. Tomita, M. Yamaguchi, and Y. Sasaki, "Evidence of nonuniform carrier distribution in multiple quantum well lasers," *Appl. Phys. Lett.* **71**, 767 (1997).

[19]B.-L. Lee, C.-F. Lin, J.-W. Lai, and W. Lin, "Experimental evidence of nonuniform carrier distribution in multiple-quantum well laser diodes," *Electron. Lett.* **34**, 1230 (1998).

[20]D.Ahn and S. L. Chuang, "Optical gain and gain suppression of quantum-well lasers with valence band mixing," *IEEE J. Quantum Electron.* **26**, 13 (1990).

[21]C.-H. Chen, C.-F. Lin, Y.-S. Su, C.-C. Huang, and B.-R. Wu, "Broadly tunable dual-wavelength semiconductor laser in optical-communication band," *CLEO2002*,Long Beach, CA, 2002, Paper CWK.